Applied Catalysis A, General 643 (2022) 118783

Contents lists available at ScienceDirect

Applied Catalysis A, General

journal homepage: www.elsevier.com/locate/apcata

Effect of catalyst surface chemistry and metal promotion on the liquid-phase ethanol condensation to higher alcohols

Laura Faba [a], Jennifer Cueto [a], Mª Ángeles Portillo [b], Ángel L. Villanueva Perales [b], Salvador Ordóñez [a,*,1], Fernando Vidal-Barrero [b]

[a] Catalysis, Reactors and Control Research Group (CRC), Dept. of Chemical and Environmental Engineering, University of Oviedo, 33006 Oviedo, Spain
[b] Departamento de Ingeniería Química y Ambiental, Universidad de Sevilla, Camino de los Descubrimientos, s/n, 41092 Sevilla, Spain

ARTICLE INFO

Keywords:
Mixed oxides
Bifunctional catalysts
1-octanol
2-ethyl-1-hexanol
Copper

ABSTRACT

The production of higher alcohols (C4+) via ethanol liquid-phase condensation is studied in this work, screening catalysts with different acid/base properties, observing similarities but also relevant differences with respect to gas-phase reactions in the gas phase. The mechanistic analysis demonstrates the relevance of acidity, mainly to promote the dehydrogenation steps. In the same way, side reactions and hydrogenations have less relevance than in gas-phase, promoting the condensations and, subsequently, obtaining heavy compounds. The highest alcohol selectivity is reached with MgAl (2/1), with more than 79% of C4+ selectivity, but the activity of this material is conditioned by the low conversion obtained. The presence of water reduces the activity because of a competitive adsorption on the catalytic sites whereas the activity increases significantly when using bifunctional catalysts. The best results, obtained with 1% Cu/MgAl (2/1), allow rising the conversion up to more than 460% respect to the parent mixed oxide, with almost 44% of the alcohol mixture enriched in heavy compounds, mainly C6 and C8.

1. Introduction

Ethanol is one of the most versatile and available biomass-derived molecules, with an increasing industrial production in the last years [1]. It is an interesting building block molecule used in the manufacture of drugs, plastics, and other compounds, both by enzymatic and catalytic routes [2–4]. Nevertheless, its main use is as biofuel, providing sustainable energy with properties close to gasoline, but its poor lubricant properties can negatively influence the engine's durability. Mixtures of ethanol with higher alcohols (mainly branched ones) can overcome this problem. The Guerbet reaction is the most promising route to obtain these second-generation biofuels [5,6]. The complex mechanism of this reaction, involving dehydrogenation, condensation and hydrogenation steps, hinders its industrial application, requiring more research to increase the selectivity. Most of the previous works have been performed in the gas-phase, with temperatures relatively high (>300ºC), defining the 1-butanol as the target compound, and reaching maximum yields lower than 30% [7–14]. Due to the extended number of side reactions, complex mixtures are obtained, being difficult to purify because of the similar physiochemical properties of most of these products.

It is expected that working in condensed phase, at high pressure and close to the ethanol critical point, the activity changes significantly and the product distribution control increases. However, there are only few studies based on the optimum conditions obtained in the gas-phase. Thus, *Riitonen and co-workers* reached selectivities towards 1-butanol up to 70%, working with different γ-Al_2O_3 supported metal catalysts, at 250ºC with 100 bar, with conversions between 10% and 30% [15–17]. Similar selectivities are reported with more complex configurations, using microwaves-assisted reaction and Ni/Al_2O_3 catalyst [18] or combining metal catalyst with homogeneous bases [19]. At the same temperature but at 176 bar, a selectivity to butanol higher than 83% is reported by *Ghaziaskar and Xu*, using 8% Ni/γ-Al_2O_3, with 35% of ethanol conversion [20]. With these bifunctional catalysts, the acid sites promote the condensation as well as the C═O hydrogenations by the Meerwein-Poondorf-Verley (MPV) mechanism whereas the metal nanoparticles enhances the dehydrogenation and C═C hydrogenation steps. The main route competes with undesired acid-catalyzed additions and different acetals and acetates are also obtained. The relevance of

* Corresponding author.
E-mail address: sordonez@uniovi.es (S. Ordóñez).
[1] Fax: + 34 985 103 434

https://doi.org/10.1016/j.apcata.2022.118783
Received 2 May 2022; Received in revised form 13 July 2022; Accepted 14 July 2022
Available online 20 July 2022

these side reactions increases with the molecular weight of the compounds, whereas the acid-catalyzed condensation decreases. Consequently, the Guerbet mechanism is limited to the first condensation (C4).

The co-presence of basic sites is expected to improve the initial dehydrogenation. This approach, scarcely studied, could be adapted to enhance the condensation step, increasing the size of the products to six and eight carbon atoms. Thus, mixed oxides have been considered, reaching selectivities of 1-butanol close to 70%, but with low ethanol conversions (<5%) [21]. *Miller and co-workers* propose a nickel supported mixed oxide (Ni/La_2O_3-γ-Al_2O_3), obtaining 41% of ethanol conversion with more than 70% of butanol [22,23].

In the last years, the industry interest has shifted to these higher alcohols since they have a high value in the production of plasticizers, soaps, and fine chemicals, in addition to their properties as solvents and fuel additives [23,24]. However, the production of these heavy alcohols from ethanol has been poorly studied. Preliminary studies in gas-phase propose a sequential configuration (from ethanol to butanol and from butanol to 2-ethyl hexanol (2EH)) with different catalysts and reaction conditions [25–29]. This configuration is quite complex from the technical point of view, because of the low selectivity of the first stage. The limited literature in liquid phase (batch configuration) proposes a maximum of 32% of conversion with selectivities of 22% of hexanol and 60% of butanol, at 230ºC, using 7–10% Cu/MgAl, with a catalyst/reactant mass ratio close to 0.1 [6,30,31]. Despite these promising results, there is a lack of systematic study that allows identifying the relevant catalytic properties and the reaction conditions to improve the selectivity to higher alcohols (>C4) and their corresponding precursors.

This work presents a comprehensive study of the liquid-phase ethanol self-condensation considering the production of heavy alcohols (C6-C8) as a one-step process. The activity of different catalysts (HAP, MgAl, MgZr, MgFe, MgCaAl) was studied analyzing the results as a function of their morphological and physic-chemical properties. These materials were chosen considering the previous literature for Guerbet gas-phase condensations, with well-recognized works highlighting the activity and selectivity of HAP [32–35] and different mixed oxides [14, 21,31]. Despite the different structures of these materials, the same type of active sites (acid and base ones) as well as their hydrogenation capacity by the MPV mechanism are highlighted as the key parameters for the reaction, allowing the comparison. The reaction conditions (no solvent, low catalytic loading) were chosen to achieve a tight control of the activity to facilitate the identification of the catalytic behavior on each single step of the process. These results are analyzed to propose a mechanism, detecting similarities and differences with respect to the gas-phase configuration. Different metals were supported on the most promising materials, analyzing if the presence of nanoparticles with hydrogenation and dehydrogenation activity have a crucial role enhancing the production of the target compounds.

2. Material and methods

2.1. Catalysts preparation

A commercial hydroxyapatite (HAP) (Sigma Aldrich) is used in this work, whereas the different mixed oxides (MgZr, MgAl, MgFe and MgCaAl) were prepared in the lab. The details of each particular preparation method are included in the Supplementary Information.

Bifunctional catalysts were prepared supporting Pt, Ni, Cu, Ru or Pd by the dry-impregnation method, using nitrate precursors. This was done by adjusting the volume of the metallic precursor solution (prepared to achieve the target 1 wt% of metal loading) to the pore volume of the support, ensuring the total impregnation and a high dispersion. The impregnated catalyst was dried for 24 h, calcined to 700 °C and reduced with a H_2 flow of 20 mL·min^{-1}, up to a temperature of 450 °C (ramp 5 °C·min^{-1}), holding this temperature for 3 h.

2.2. Catalysts characterization

The catalytic morphology was determined by N_2 physisorption, using a Micromeritics ASAP 2020 instrument, applying the BET and BJH methods to calculate the surface area, the pore diameter and volume. The crystalline phases were analyzed by X-ray diffraction (PANalytical X′Pert Pro), working with the Cu-Kα line (0.154 nm) in the range $2\theta = 10 - 120^{\circ}$. These analyses were done with fresh and spent materials to identify possible changes in the structure during the reaction.

The acidity and basicity quantifications (fresh and spent catalysts) were performed by a programmed temperature desorption (TPD) in a Micromeritics AutoChem II 2920, following the desorption of the probe molecules (NH_3 or CO_2) by a Pfeiffer Vacuum-300 mass spectrometer. A previous cleaning step with He ensures the absence of physisorbed compounds. The saturation was done for 20 min with a 20 mL·min^{-1} flow (2.5% NH_3 in He or 99.5% of CO_2). The desorption was monitoring from room temperature to 950ºC, with a slope of 5 ºC·min^{-1}.

The evolution of the catalytic surface with the reaction was analyzed by diffuse reflectance infrared spectra using a Thermo Electron Nicolet FTIR spectrometer equipped with a MCT/A detector. Spectra were recorded in the 4000–1200 cm^{-1} range, with a resolution of 4 cm^{-1}, collecting 256 scans/spectrum. 20 mg of catalyst were used in each experiment, being placed inside a high temperature cell. Catalytic measurements were conducted at 230ºC under inert atmosphere (N_2 flow of 20 mL·min^{-1}) or under an atmosphere saturated in ethanol.

The metal loading of the bifunctional catalysts was determined by Inductively Coupled Plasma Mass Spectrometer (ICP-MS) using a HP 7900 of Agilent. Approximately 50 mg of the sample were inserted into a microwave-assisted Teflon bomb; adding HCl (2.25 mL) and HNO_3 (0.75 mL) to dissolve the sample. The metal dispersion and particle size distribution was quantified by transmission electronic microscopy (TEM) using a MET JEOL 1011. Histograms and average particle size were calculated by analyzing 100 particles in each sample, using the software Confocal ImageJ.

2.3. Catalytic performance

The ethanol condensation was performed in a 0.5 L stirred batch autoclave reactor equipped with a PID temperature controller and a backpressure regulator (Autoclave Engineers EZE Seal). Firstly, 200 mL of ethanol (EtOH) (VWR, 100%) and the catalyst (0.5 or 2 g as a function of the experiment) was added to the reactor. The air was purged with N_2, and condensation was carried out at 230 °C, under 30 bar of N_2 (pressure at room temperature, increasing to 80 bar at 230 °C) under stirring (1000 rpm) for 8 h. This temperature is the average of those reported in the bibliography (from 200 to 250ºC) [6,22,23,31], considering the limit conditions allowed by the reactor. Based on these points, the conditions were selected as an equilibrium that guarantees the liquid state of all the compounds involved, the conditions that could promote the reaction to heavier compounds (>C4) as well as the minimum severity of the reaction, in good agreement with the desired sustainable character of the process.

A filter placed inside the sampling port prevents the catalytic extraction during the sampling. The evolution of the different compounds involved in the reaction was analyzed by gas chromatography (GC) in a Shimadzu GC-2010 equipped with a FID detector, using a 30 m long CP-Sil 8 CB capillary column. Peak assignment was carried out by GC-MS in a Shimazdu GC/MS QP 2010 Plus Instrument, using a 30 m long TRB-5MS capillary column. EtOH and the majority peaks calibrations were done using commercial samples, whereas minority products calibration was carried out using the relative carbon concept proposed by Scanlon and Willis [36]. The analytical conditions (detailed in the Supplementary Information, Table S1) were chosen to guarantee that the ethanol signal does not saturate the detector, even in the case of initial samples (the highest signal expected). Each reported experimental point corresponds to the average value of at least two analyses.

The maximum standard deviation of the reported values is 6%. The results were analyzed in terms of conversion, selectivities, and carbon balance, according to Eqs. (1), (2), and (3), where "n_i" corresponds to the number of carbons in each compound, and "$C_{i,t}$" is the molar concentration of this compound at the time analyzed:

$$Selectivity: \quad \varphi(\%) = \frac{n_i \cdot C_{i,t}}{2 \cdot \left([EtOH]_0 - [EtOH]_t\right)} \cdot 100 \tag{1}$$

$$Conversion: \quad x \quad (\%) = \frac{[EtOH]_0 - [EtOH]_t}{[EtOH]_0} \cdot 100 \tag{2}$$

$$Carbon \quad Balance: \quad CB = \frac{\sum n_i \cdot C_{i,t}}{2 \cdot [EtOH]_0} \tag{3}$$

At reaction conditions, the presence of solid deposits is discarded (assumption corroborated by TPO analyses). The differences in carbon balance closures are then attributed to the formation of light compounds, not detected in the liquid phase. This hypothesis was corroborated by the analysis of the gas phase, being recovered using a sampling bag. The gases accumulated were analyzed by GC-MS. Only a qualitative analysis is possible, the quantification and temporal evolution evaluation being not possible due to the accumulative sampling required.

The accuracy of GC-FID analyses in these conditions was probed analyzing ethanol signal and the standard deviation of 12 repetitions of the same sample, as indicated in the Supplementary Information (see Table S2). The values indicated are congruent with the theoretical conversion required to obtain the products detected. However, this second methodology is discarded with the aim to compare the relevance of permanent gases produced in the reactions, analyses that could be not possible if the conversion is calculated based on products.

3. Results and discussion

3.1. Catalyst screening

Initial experiments were focused on the comparison between bulk materials to identify the catalytic properties that maximize the selectivity to higher alcohols, mainly C6 and C8, or their corresponding condensed precursors (in absence of metal particles with hydrogenation activity). In all the cases, anhydrous ethanol was used as reactant, setting the temperature at 230ºC. The evolution of ethanol conversion with time is analyzed in Fig. 1.

The absence of an external solvent (high reactant initial concentration, 789 g·L^{-1}) as well as the low catalytic loading (2.5 g/L) justifies the conversions obtained. Similar conversions are reported in most of the previous literature when working without external solvent, even with higher catalytic loading [14,17,21,23]. In fact, comparing the results in terms of mass of ethanol reacted per time and catalyst loading, the values obtained in this study (from 0.473 to 0.907 g/g·h with MgZr and MgAl (3/1), respectively) are better than most of those drawn from studies in absence of reduced metals (0.710 g/g·h [14,30], 0.647 g/g·h [21]), with the exception of *Perrone and co-workers*, who obtained values of 1.326 g/g·h with a partial substitution of Mg^{2+} and Al^{3+} by Cu^{2+} and La^{3+}, respectively [31].

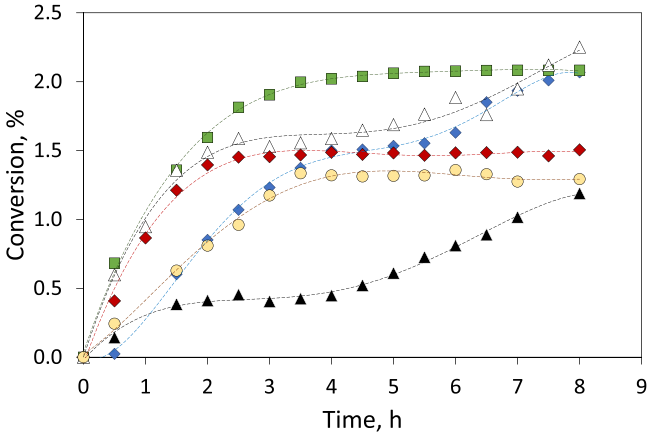

Fig. 1. Evolution of the pure ethanol conversion at 230ºC as a function of the catalyst (0.5 g). Symbols: (◆) HAP, (■) MgFe, (▲) MgZr, (△) MgAl (3/1), (◆) MgAl (2/1), (●) MgCaAl.

Although higher conversions could be anticipated working with higher catalytic loading, reported conversions are more useful for gaining further understanding on reaction mechanism and the role of the different surface sites. MgZr shows the poorest activity, maximum conversion of 1.2% after 8 h, suggesting that longer times could rise this value because of the increasing trend observed. Low conversions (1.3–1.5%) are also reached with MgAl (2/1) and MgCaAl, but in these cases, the values remain almost constant after the first 2 and 3 h, respectively. On the other hand, conversions obtained with HAP, MgFe and MgAl (3/1) are significantly higher, with values from 2% to 2.3%. As in the previous case, three different trends are observed, with a constant conversion in less than 2 h with MgFe, a continuous evolution observed with HAP, and an intermediate behavior of MgAl (3/1), with a fast increase during the first 2 h and a second and slower increasing trend at longer times after an intermediate and flat step.

Table 1 summarizes the product distributions after 8 h reaction time, in terms of absolute and relative selectivity of main families of compounds. Considering the large number of products obtained, the absolute selectivities are lumped by families, according to their number of carbons. Thus, C2 only involves the acetaldehyde, whereas C4 corresponds to crotonaldehyde, butanal, and 1-butanol, with a similar distribution for C6 and C8 families. Although quantitatively analyzed, side products (as esters) are not included in these families, being considered together as "undesired liquid by-products". Reported carbon balance closure is calculated comparing the initial ethanol loading and the concentration of ethanol and all the desired and undesired reaction product analyzed in the liquid phase after performing the reaction. Although this carbon balance closure is very high, as the ethanol conversions are low, selectivity to gas products can be important. Thus, apparent selectivities to gaseous by-products have been estimated from ethanol conversion and carbon balance, being these values also reported

Table 1
Summary of the results after 8 h of ethanol liquid-phase condensation at 230ºC using different catalysts.

	HAP	MgFe	MgZr	MgAl (3/1)	MgAl (2/1)	MgCaAl
Selectivity (%)						
C2	13.3	2.3	7.8	3.6	2.5	6.4
C4	40.2	0.1	18.1	1.0	78.6	14.3
C6	2.4	2.9	7.6	3.0	11.3	23.7
C8	0.1	–	–	0.1	1.4	2.1
Alcohols (%)	**34.9**	**0.1**	**14.2**	**0.7**	**79.1**	**14.1**
Butanol	*99.7*	*100*	*90.7*	*92.7*	*98.6*	*78.6*
3-Hexen-1-ol	–	–	–	–	*0.1*	*3.4*
Hexanol	*0.3*	–	*9.3*	*4.9*	*0.5*	*9.8*
2-Etil-1-hexanol	–	–	–	–	*0.3*	*4.7*
1-Octanol	–	–	–	*2.4*	*0.5*	*3.8*
Aldehydes (%)	**21.0**	**5.2**	**19.3**	**6.9**	**14.8**	**32.9**
Acetaldehyde	*77.2*	*70.4*	*50.7*	*75.0*	*36.7*	*42.1*
Crotonaldehyde	*9.9*	–	*29.4*	*3.4*	*10.2*	*12.9*
Butanal	*1.2*	–	*0.2*	–	*2.0*	*1.7*
Hexanal	*15.7*	*29.6*	*19.7*	*20.9*	*50.3*	*43.2*
2-ethyl-hexanal	–	–	–	*0.2*	*0.7*	*0.2*
Undesired liquid by-products	*7.7*	*6.8*	*7.6*	*8.1*	*6.1*	*10.5*
Gaseous by-products	*36.3*	*87.9*	*58.9*	*84.2*	*0.1*	*42.5*
Carbon Balance (%)	*99.8*	*98.2*	*99.4*	*98.1*	*99.8*	*99.4*

in Table 1.

As anticipated, the liquid-phase configuration promotes a different distribution than the gas-phase one, with a decrease of C4s in favor of a higher number of heavy compounds (C6 and C8), mainly observed with MgAl (2/1) and MgCaAl. These compounds are the heaviest detected in this study, concluding that subsequent dehydrogenations and/or aldolizations require more severe conditions. In the gas-phase reactions, only some traces of C6s are detected using bimetallic modified mixed oxides [31,43].

More than 26% of the total compounds correspond to C6 and C8 when using MgCaAl, the best catalyst promoting condensation. In the case of MgAl (2/1), this percentage decreases to one half of this value. In terms of functional groups, MgAl (2/1) shows a high hydrogenation activity, alcohols representing almost 80% of the total. On the other hand, with MgCaAl, alcohols only correspond to 14%, suggesting that condensation prevails over hydrogenation. In both cases, all the C6-C8 alcohols are obtained following the same ratio as the carbon families. Regarding the aldehydes, both materials produce hexanal, which hardly condensates with other ethanol molecule, limiting the production of C8s.

C6 are the heaviest compounds detected with MgZr (7.6%). A similar distribution of aldehydes and alcohols is obtained. The high concentration of crotonaldehyde (almost 30%) with respect to butanal (almost negligible) suggests that the C═O hydrogenation is easier than the C═C one, most of the butanal being directly converted into butanol.

HAP, MgFe, and MgAl (3/1) do not show relevant activity for heavy condensations, with less than 3% of C6 and C8 compounds. In the case of HAP, the results are congruent with a lack of activity promoting the condensation of heavy compounds, obtaining a sample enriched in C4 (>40%) with a good balance between aldehydes and alcohols (35% of butanol). On the contrary, MgFe and MgAl (3/1) demonstrate a poor condensation activity, with total selectivities lower than 10%, producing almost 90% of undesired gases (ethylene and diethyl ether).

To sum up, these materials reveal differences not only in terms of conversion but also in the product distribution. The instability of some of the catalysts at reaction conditions could be a possible justification of these discrepancies. IPC results indicate the absence of metals in the reaction liqueur since Mg, Al, Ca, Fe or Zr are not detected. The catalytic leaching is then discarded as a deactivation cause. On the other hand, the comparison between crystallographic phases of fresh and spent materials (XRD diffractograms shown in Fig. S1 and Table S3, discussed below) reveals a good correspondence between peaks before and after the reaction, prevailing the amorphous structure of these materials, without observing the parent hydrotalcite structure (crystalline one). Thus, the physical and morphological stability of these materials is also corroborated. In this context, a relevant role of their catalytic properties is suggested, promoting different steps of the main mechanism, preventing undesired lateral reactions, and minimizing the adsorption of different compounds. This discussion requires the analysis of the morphological and physico-chemical properties of these materials, main data being summarized in Table 2.

Morphological results discard any relevant role of the external surface area or mass transfer limitations. In general, materials with a fast initial conversion (MgFe, MgAl (3/1), MgAl (2/1)) exhibit high concentration of acid sites (mainly weak and medium ones), whereas materials with a lower acidity require longer times. These results demonstrate the relevance of acid sites adsorbing the ethanol molecule. This conclusion was verified by DRIFT spectroscopy, observing more pronounced bands with MgAl (3/1), the most acidic material. The identification of all the DRIFT bands, based on previous literature [37,38], as well as their discussion, is detailed in Fig. S2.

MgAl (2/1), MgCaAl, HAP and, in a small extent, MgZr have the highest capacity to promote the condensation, in agreement of their high concentration of medium and strong basic sites, releasing water. Previous literature indicates that some oxides derived from a hydrotalcite-type precursor undergo rehydration in presence of water, modifying their surface chemistry by the reconversion of the O^{2-} basic sites to OH^- ones (Brønsted sites responsible of aldol condensations) [39]. This hydration depends on their surface structure and can also occur with HAP [40]. This fact would be enough to increase its condensation capacity, not so relevant to observe differences in the crystallographic structure (surface phenomenon). This effect was corroborated by comparing the acidity and basicity of fresh and spent catalysts. Results obtained (shown in Figs. S3-S4 and Table S4) indicate the relative enrichment in medium-strength basic sites of MgZr and HAP, the materials that suffer reactivation, whereas the strength of acid sites remains almost invariable, resulting in stronger basic/acid pairs. According to the literature, these sites promote the dehydrogenation of ethanol via E_{1cb} elimination mechanism [41], justifying the reactivation observed with these materials. This reactivation has not been reported in gas-phase reactions, suggesting that Brønsted sites are not stable at high temperatures.

A similar reactivation and increase in the basic/acid sites strength is observed with MgAl (3/1), but it shows low condensation capacity (5% of >C2). This fact is justified by the lack of correlation between basic/acid pairs, prevailing the activity only catalyzed by acidity. In this case, water is released by undesired acid additions (yielding 1,1-diethoxyetane, selectivities up to 8%) and ethanol dehydrations, producing ethylene and diethyl ether in large amount (>84%). These two compounds were identified in the analysis of the gas phase by GC-MS. In good agreement with their presence, the carbon balance closure with this material (98.1%) is the lowest one. In other materials, a clear decrease in the acidity without a relevant change in the strength distribution is observed (43%, 61%, and 62% with MgAl (2/1), MgFe, and MgCaAl, respectively). With these materials, the expected rehydration effect is shielded by the adsorption of unsaturated intermediates, severely blocking the acid sites and hindering further reaction progresses.

The different profiles of the two MgAl mixed oxides deserves special attention, suggesting a strong influence of the preparation method and the Mg/Al ratio. The minor differences in terms of weak and medium-strength acidity discard a different dehydrogenation capacity. In fact, the conversions during the first 3 h are very similar. XRD diffractograms (Fig. S1) illustrate relevant differences, consequences of the interaction between oxide phases during the preparation. In good agreement, a spinel (MgAl, JCPDS 00–021–1152) is detected in MgAl (2/1), in addition to periclase (MgO, JCPDS 03–065–0476), the only phase observed with MgAl (3/1), suggesting that Al is in an amorphous phase or in crystals too small to be identified with the resolution of this equipment. The different coordination state of Mg and Al on these crystalline phases (and the corresponding morphology of the acid sites) seems to play a key role in the interaction of reaction intermediates with the catalysts, producing opposite effects in the catalytic activity. DRIFT spectra (Fig. S2) visualize these differences. Thus, signals of ethoxide species (1460 cm^{-1} [42]) are significantly more evident in the case of MgAl (3/1) than in MgAl (2/1).

Table 2
Surface and physicochemical properties of the different catalysts. Results corresponding to N_2 physisorption and NH_3 and CO_2-TPD.

	HAP	MgFe	MgZr	MgAl (3/1)	MgAl (2/1)	MgCaAl
S_{BET} ($m^2 \cdot g^{-1}$)	48	215	111	262	179	52
d_p (nm)	17	18	18	16	8	24
Total acidity ($\mu mol \cdot g^{-1}$)	**1086**	**2165**	**735**	**2692**	**1857**	**1635**
Weak (<250ºC)	157	1374	227	872	726	662
Medium	572	568	331	1150	959	747
Strong (>500ºC)	357	223	177	670	172	226
Total basicity ($\mu mol \cdot g^{-1}$)	**1363**	**304**	**498**	**478**	**716**	**1659**
Weak (<250ºC)	335	122	363	305	185	224
Medium	204	68	118	110	441	1100
Strong (>500ºC)	824	114	17	63	90	355

The reaction products from the two materials with the lowest weak acidity (HAP and MgZr) are enriched in acetaldehyde, suggesting that these sites are involved in the condensation, directly by an acidic mechanism ore stabilizing the basic sites (basic/acid pairs). The high acidity justifies the poor results obtained with MgAl (3/1) and MgFe, with more than 84% of carbon as gaseous by-products. The sampling method for the analysis of these gases does not allow accurate and continuous quantification, but in both cases more than 90% corresponds to ethylene, with lower amounts of diethyl ether and other compounds in traces. These results contrast with those obtained with MgAl (2/1), material that prevents the formation of gaseous by-products. The high acidity of this material is well balanced with its basicity, suggesting the primacy of basic/acid pairs over isolated acid sites, promoting the main route of the Guerbet reaction.

There is a good correspondence between the medium-strength basic/acid sites and the total selectivity to C6 and C8 compounds, indicating that these sites are the most relevant ones to promote condensations, as induced from the total C6-C8 selectivity of MgCaAl (25.8%) and MgAl (2/1) (12.7%). Even with this amount of C6 and C8, MgAl (2/1) produces the maximum amount of C4 (78.6%), followed by HAP (40.2%), being suggested as promising supports for next studies. These catalysts produce the maximum total alcohol selectivity, being enriched in butanol.

Thus, the conversion is not always related with a high activity in the Guerbet reaction since also undesired ethanol dehydration and acid-catalyzed additions occur, obtaining light gases. MgFe and MgAl (3/1) produce selectivities to diethoxyethane at initial times higher than 9.7% and 10.4% (values that corresponds to relative weights of 39% and 24% of this compound in the products' mixture), respectively. Only in the case of MgAl (2/1), this conversion corresponds to desired products, observing 1-butanol since the first samples.

To explain these results, a separate experiment with MgAl (2/1) and pure butanol as reactant was done. The evolution of the main intermediates is detailed in Fig. S5. Less than 1.7% of conversion is reached after 8 h (99.8% carbon balance), with ethanol and butanal (16.3%) as the main reaction products and less than 1% selectivity for C6s and C8s (0.2% 3-hexen-1-ol, 0.4% of 1-hexanol, 0.2% of 2-etil-1-hexanol). Thus, the C6 adducts are suggested to be produced mainly by the condensation between crotonaldehyde and acetaldehyde, but not so easily from butanal (the selectivity of this compound is more than 20 times higher than when using ethanol). Thus, once crotonaldehyde is partially hydrogenated to butanal, the condensation capacity decreases. This hypothesis is congruent with the stability of the enol intermediate produced during the condensation in presence of C═C double bonds. The quantification of acetaldehyde and ethanol suggests a partial reversible character of condensation not observed in gas phase or when ethanol is used as reactant since the reverse reaction is catalyzed by the same active sites than the direct one, the condensation prevailing in presence of aldehydes. According to this study, strong acid sites and basic/acid pairs are required to promote the butanol double dehydrogenation and condensation. Their low concentration as well as the adsorption of the C6 and C8 compounds with the subsequent active-sites blockage conditions the low second condensation ability and justifies the prevalence of hydrogenated C4 compounds.

In all the cases, the hydrogenation capacity decreases with the size of the aldehydes. This is an anticipated result considering the absence of metal nanoparticles and the prevalence of the MPV route. According to this mechanism [8], the hydrogenation requires the co-adsorption of the aldehyde and an alcohol, on an acid site, obtaining a cyclic compound as the reaction intermediate. The stability of this intermediate decreases with the size, being the most unstable the one of six carbons (crotonaldehyde + ethanol). Thus, the ratio of butanol to the total C4 family of compounds reaches values higher than 99% with Mg/Al (2/1) whereas this percentage decreases to 45% when analyzing the C8 hydrogenation capacity.

To establish a reaction mechanism, these results after 8 h must be analyzed together with the evolution in time of the different intermediates. The most relevant data are shown in Fig. 2, excluding MgFe and MgAl (3/1) because of their negligible condensation activity.

Acetaldehyde is the first intermediate obtained with all the materials, with initial selectivities of 100% and a continuous decreasing trend with the time. This decreasing trend is more marked in those catalysts with higher condensation activity. According to these results, the ethanol dehydrogenation to obtain acetaldehyde is the starting point of the process, discarding the direct coupling between two ethanol molecules as a relevant step. Despite the lack of total agreement about the ethanol condensation in gas-phase, this mechanism prevails in the literature over the ethanol direct condensation [25,44].

The typical evolution of a successive condensation C4-C6-C8 is observed with MgZr and, being not so marked, with HAP. With these two materials, C4s and C6s compounds reach a maximum in selectivity, slightly displaced in conversion in the case of C6s, according to their intermediate character. The high hydrogenation activity of MgAl (2/1) alters these curves, observing a high accumulation of C4s due to the stable character of butanol. The high condensation activity of crotonaldehyde is observed with MgCaAl, material with which C4s and C6s almost appear simultaneously, with a high proportion of the last ones, consuming most of the crotonaldehyde obtained in the first condensation.

As to the evolution of each intermediate, a first hydrogenation of C═C bonds is observed for the C4 family (Fig. 3a), suggesting a consecutive production of butanal and butanol that is assumed to be extrapolated to heavier compounds (C6 and C8). The C═O hydrogenation by the MPV mechanism as well as the subsequent condensations justify the low selectivity to these aldehydes, with a fast production of heavy compounds or alcohols once these intermediates are obtained. The slow but continuous hydrogenation activity of these materials (see Fig. 3b) suggests that longer times could enhance the selectivity of these target compounds with all the catalysts except MgFe and MgAl (3/1) because of their lack of condensation activity.

According to these results, the basis of the mechanism in the liquid phase is based on the one in the gas phase but with some modifications. Different side reactions are observed (ethoxides not detected in gas phase and quite relevant in the liquid one). The softer conditions of this configuration and the absence of noble metals justify the slow rates of hydrogenations, increasing the opportunity to obtain heavier chemicals by the condensation of unsaturated compounds. The presence of isomers as well as partially hydrogenated derivatives rises the total number of compounds. Considering the experimental results, the scheme proposed for the liquid-phase ethanol condensation can be updated to a more complex one considering the different compounds detected with more than four carbon atoms, as shown in Scheme 1. In this scheme, the different isomers that could be simultaneously obtained are indicated, as well as the fact that C8s are produced by the sequential addition of an acetaldehyde molecule to crotonaldehyde, the direct condensation of two crotonaldehyde molecules or the condensation involving butanal being discarded as relevant at these conditions.

The temporal evolution of reaction products also supports the previously mentioned required trade-off between hydrogenation and condensation activity, the fraction of heavy compounds reaching a maximum with those materials highly selective to alcohols, whereas observing a slow but continuous increasing trend with MgAl (2/1) and HAP, as shown in Fig. 4. These results indicate that higher selectivities can be obtained modifying the reaction conditions.

3.2. *Influence of the catalytic loading*

According to the preliminary analysis, a higher catalytic loading is anticipated to have a positive influence on the product carbon-length if the condensation activity prevails over the hydrogenation one. To check this hypothesis, the results obtained with 2.5 g/L are compared with those reached using 10 g/L. Once the catalytic loading is increased, the

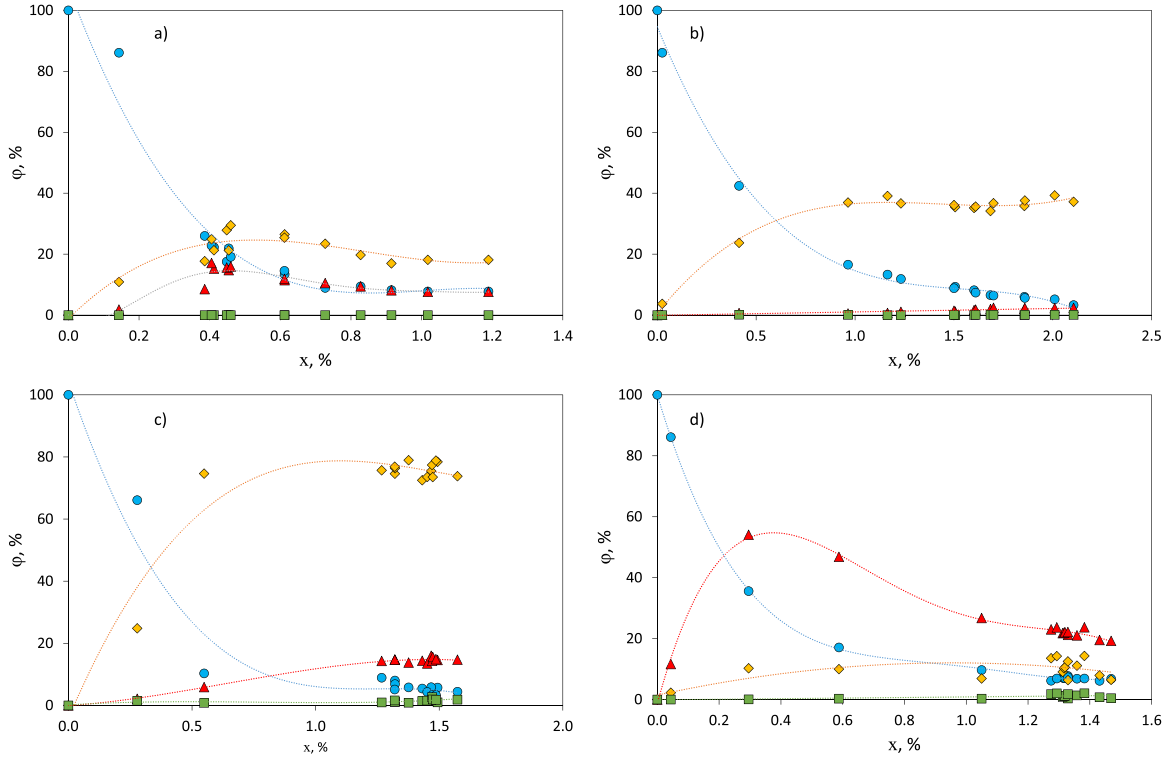

Fig. 2. Evolution of the selectivities versus conversion in the ethanol condensation at 230ºC with (a) MgZr; (b) HAP; (c) MgAl (2/1); (d) MgCaAl. Symbols: (●) C2; (◆) C4; (▲) C6; (■) C8.

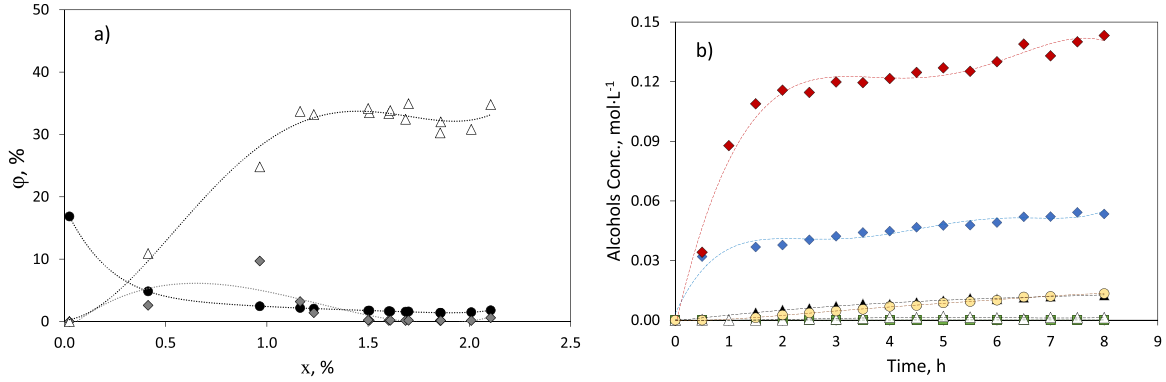

Fig. 3. : (a) Selectivity evolution of (•) crotonaldehyde, (◆) butanal, and (△) butanol as a function of the ethanol conversion obtained with HAP at 230ºC. (b) Temporal evolution of alcohols concentration during the ethanol condensation at 230ºC with different catalysts. Symbols: (◆) HAP, (■) MgFe, (▲) MgZr, (△) MgAl (3/1), (◆) MgAl (2/1), (●) MgCaAl.

conversion is 160% higher with MgAl (2/1), from 1.5% to 3.9% (with a continuous increasing trend during the 8 h), whereas a lower increase from 2.1% to 2.9% is observed with HAP (flat conversion after 5 h). However, the main differences are related to the selectivity distribution, compared in Fig. 5.

There is an increase in the selectivity of the C6s, in detriment of the C4s and, in the case of the HAP, of acetaldehyde too. The amount of C8 compounds is negligible in both cases, suggesting that stronger sites are required to promote this step. The increase in the condensation activity is in detriment to the hydrogenation one. This is congruent with the decreasing stability of MPV intermediates with the size of the intermediates, as discussed before. Thus, hydrogenated compounds decreased from 79.1% to 35% MgAl (2/1), whereas the initial 34.9% reached with 2.5 g/L of HAP declines to 10.4% with 10 g/L. In both cases, these reductions are proportional to the increases in C6s. Butanol is the main alcohol in both cases, 30.9% and 9% with MgAl (2/1) and HAP, with only 2.9% and 1.4% of hexanol, respectively. No significant differences in terms of side products were observed with any of these materials (selectivities from 6% to 11%), being more than 80% due to the 1,1-dietoxiethane, the side product obtained by the ethanol dimerization. On the contrary, the control over the reaction decreases, observing 19.2% (MgAl (2/1)) and 55.4% (HAP) of undetected gases.

Results obtained with MgAl (2/1) (>71% of target compounds) are significantly better than those reached with HAP, suggesting a good

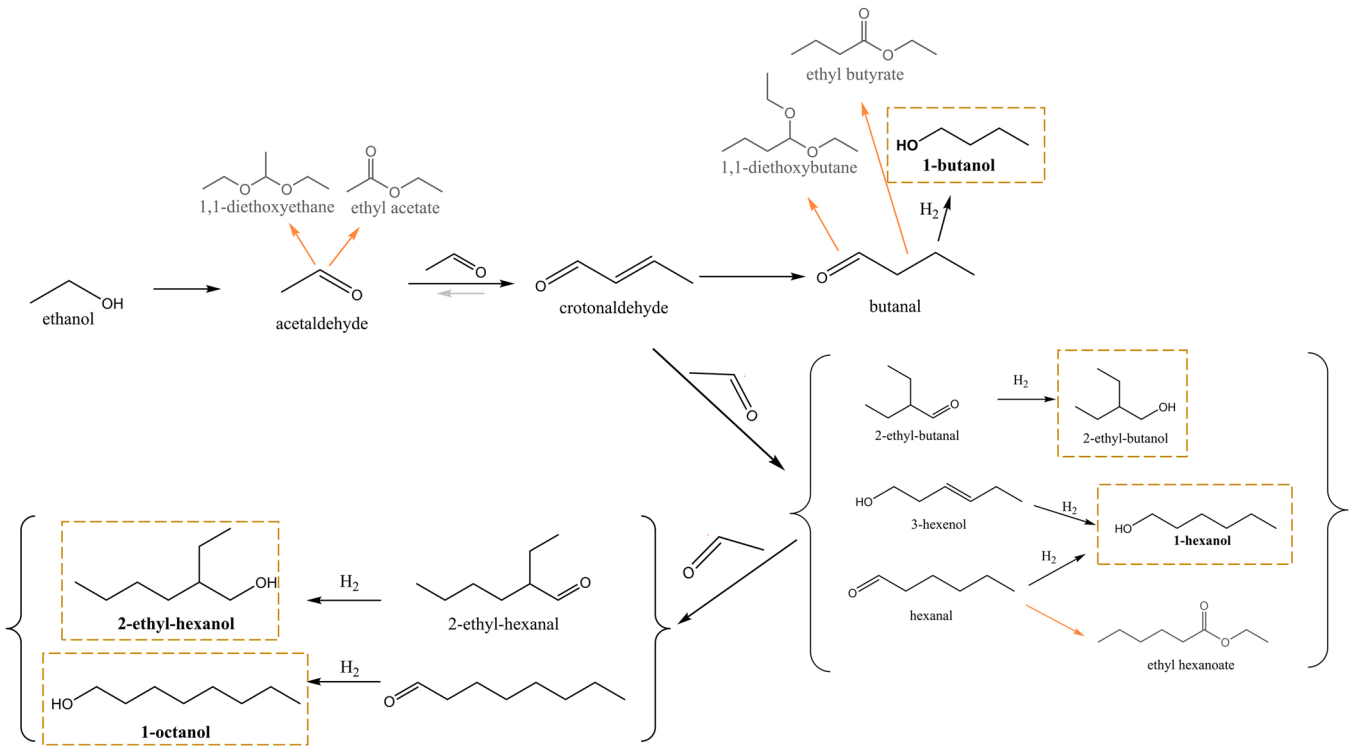

Scheme 1. Proposed scheme for the ethanol liquid-phase condensation.

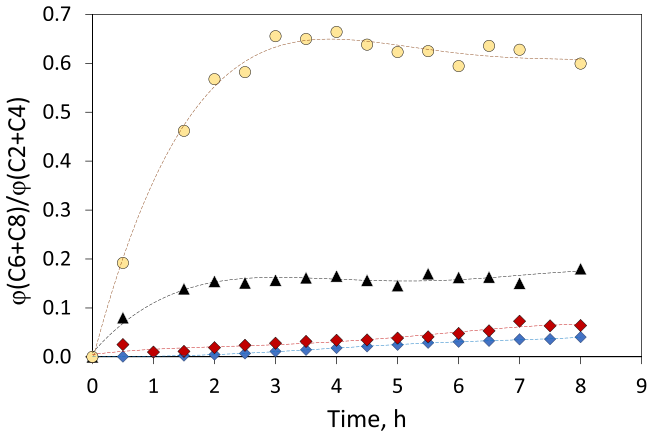

Fig. 4. Evolution of the relative weight of selectivity to higher compounds (C6 + C8) during the ethanol conversion at 230ºC as a function of the catalyst. Symbols: (◆) HAP, (▲) MgZr, (◆) MgAl (2/1), (●) MgCaAl.

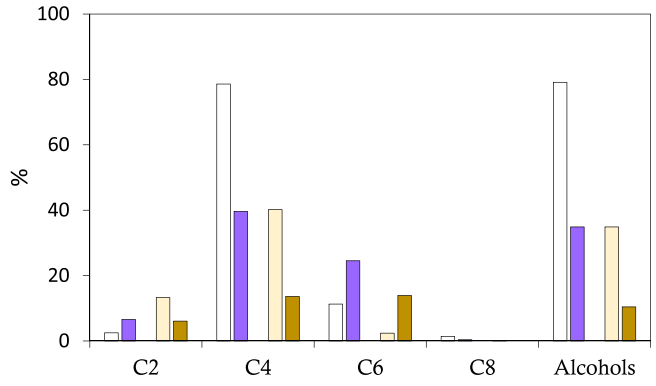

Fig. 5. Product selectivities after 8 h of ethanol liquid-phase condensation at 230ºC and 30 bar of N_2 using MgAl (2/1) as catalyst with a loading of 2.5 g/L (white) and 10 g/L (purple); or HAP, 2.5 g/L (yellow), 10 g/L (brown).

alcohols production by a second hydrogenation step. The poor increase of activity observed with HAP suggests that the positive effect of rehydration has a limited impact, and the results are mainly conditioned by other aspect, whose negative role is more evident as the reaction advances. In this context, previous literature suggests that water can play a double role, with a negative influence if the interaction with the catalyst occurs via adsorption on the strong sites [43].

3.3. Role of water on catalyst performance

The analysis of the influence of water content is of great interest, from the catalytic point of view and to evaluate the technical-economic viability of this process. As to the mechanism, it allows to identify the rate determining step. As to the technical approach, the use of aqueous ethanol is preferred in terms of costs since anhydrous ethanol is more expensive due to the required additional dehydration steps. Simple separation processes such as distillation allow reaching a maximum ethanol purity of 95% (v/v), limited by the minimum-boiling ethanol-water azeotrope, requiring expensive technologies (azeotropic distillation with benzene or cyclohexane, distillation combined with adsorption) to fully remove water from ethanol.

The results obtained in absence of water (anhydrous ethanol used as reactant) were compared to those introducing 2.5% and 5% (v/v) of water. Main results after 8 h are summarized in Table 3. Results in terms of ethanol conversion seem to be not very conclusive, with some materials for which the water promotes it (an increase in conversion of 44% observed with MgAl (3/1)), and materials with the opposite trend, more evident with HAP and MgFe (decreases of 52% and 60%, respectively). An intermediate situation is observed with MgAl (2/1), with almost constant conversion despite the water content.

These results corroborate that water preferentially interacts with the catalysts via dissociative adsorption on the strong sites, producing the

Table 3
Influence of the water percentage on the conversion and selectivity distribution.

	HAP		MgFe		MgAl (3/1)			MgAl (2/1)		
Water (%)	**0**	**5**	**0**	**5**	**0**	**2.5**	**5**	**0**	**2.5**	**5**
Conversion (%)	2.11	1.01	2.07	0.84	2.25	2.35	3.24	1.58	1.3	1.25
Selectivity (%)										
C2	13.3	17.4	2.3	17.2	3.6	14.1	33.5	2.5	18.2	13.7
C4	40.2	0.6	0.1	0.7	1.0	2.9	1.4	78.6	2.4	0.7
C6	2.4	0.2	2.9	1.9	3.0	6.5	3.1	11.3	12.9	1.9
C8	0.1	–	–	–	0.1	–	–	1.4	0.1	–
Alcohols (%)	**34.9**	**0.1**	**0.1**	**0.3**	**0.7**	**1.0**	**0.2**	**79.1**	**1.0**	**0.2**
Butanol	*99.7*	*0.1*	*100*	*100*	*92.7*	*100*	*100*	*98.6*	*100*	*100*
3-Hexen-1-ol	–	–	–	–	–	–	–	*0.1*	–	–
Hexanol	*0.3*	–	–	–	*4.9*	–	–	*0.5*	–	–
2-Etil-1-hexanol	–	–	–	–	–	–	–	*0.3*	–	–
1-Octanol	–	–	–	–	*2.4*	–	–	*0.5*	–	–
Aldehydes (%)	**21.0**	**18.1**	**5.2**	**19.5**	**6.9**	**22.4**	**37.8**	**14.8**	**32.6**	**16.1**
Acetaldehyde	*77.2*	*96.1*	*70.4*	*88.2*	*75.0*	*62.9*	*88.6*	*36.7*	*55.8*	*85.1*
Crotonaldehyde	*9.9*	*2.2*	–	*2.1*	*3.4*	*4.5*	*2.0*	*10.2*	*1.5*	*2.5*
Butanal	*1.2*	*0.1*	–	*0.4*	–	*3.6*	*1.2*	*2.0*	*3.4*	*0.6*
Hexanal	*15.7*	*0.6*	*29.6*	*9.3*	*20.9*	*29.0*	*8.2*	*50.3*	*39.3*	*11.8*
2-ethyl-hexanal	–	*0.6*	–	–	*0.2*	–	–	*0.7*	*0.3*	–
Undesired liquid by-products (%)	**7.7**	**6.1**	***6.8***	**8.8**	***8.1***	**9.0**	**15.0**	***6.1***	**9.4**	**6.2**
Undesired gaseous by-products (%)	**36.3**	**75.7**	***87.9***	**71.5**	***84.2***	**67.5**	**47.0**	***0.1***	**57.0**	**77.5**
Carbon Balance (%)	***99.8***	***99.2***	***98.2***	***99.4***	***98.1***	***99.1***	***98.5***	***99.8***	***99.5***	***99.1***

deactivation of the materials. This phenomenon has been previously reported by *Miller and co-workers* [45]. Thus, Lewis strong basic sites (O^{2-}) are converted into weaker Brønsted sites (OH^-), modifying the catalytic activity of these materials [6,14,46]. At the same time, Lewis acid sites are blocked by the adsorption of hydroxyl anions. In fact, the activity decreases in those catalysts that have the highest concentration of strong basic sites. The increase in the activity observed with MgAl (3/1) is explained by the lowest dissociation due to the lowest strong basicity (prevailing the molecular adsorption), and the subsequent lower blockage of the acid sites that promote the dehydrogenation.

The condensation capacity is also altered, enriching the final mixtures in acetaldehyde (more than 60% in all the cases), observing a total disappearance of C8 compounds and a very significant decrease in C6 and C4 condensed ones. A reduction in the condensation capacity is observed with all the materials. This result is congruent with the adsorption of water on the condensation active sites, preventing the advance of the reaction. Thus, in presence of water, the Guerbet reaction is limited by the condensation step and, even in those cases in which the ethanol dehydration is promoted, there is not a clear advance to the target compounds.

Acid sites are also involved in the hydrogenation by MPV mechanism. In good agreement, their blockage explains the almost total absence of alcohols even when feeding only 2.5% of water. This situation affects to all the fractions, observing only traces of butanol (lower than 1% in all the cases), with a total disappearance of C6 and C8 alcohols, even in those cases when the corresponding condensated adducts are still produced in significant amount, such as in the case of both MgAl materials.

Water also promotes the production of 1,1-diethoxyethane, except for HAP, with a constant selectivity of 5.6% with and without water. This acetal is obtained by the reaction between an alcohol and an aldehyde molecule, and it has been observed in the literature with selectivities close to 40% in presence of acid materials [14]. With these basic-acid materials, its selectivity reaches a maximum of 14.1% with MgAl (3/1) and 5% of water. In all the cases, this compound represents more than 90% of the total undesired products detected.

To sum up, a negative influence of free water is demonstrated, in agreement with the conclusions obtained in gas-phase, even with those catalysts showing reactivation in presence of the small amount produced during the reaction. Thus, the typical percentage of water presents in an azeotropic ethanol inhibits the reaction. Considering the increase in costs, the economic viability requires an improvement in the selectivity towards the target alcohols. The hydrogenation via the MPV mechanism is not enough to promote it, suggesting the use of bifunctional catalysts to activate the hydrogen produced during the dehydrogenation.

3.4. *Bifunctional catalysts*

Improving the dehydrogenation, the excess of acetaldehyde is expected to promote the condensations. Among the transition metals, the dehydrogenation activity of Cu is highlighted in the literature [47]. On the other hand, alcohols are produced by hydrogenation steps. The presence of noble metal nanoparticles could have a positive effect activating the hydrogen produced during the dehydrogenation, enhancing the hydrogenation activity [5]. This section analyzes the activity of different bifunctional catalysts (Cu, Ru, Pd, Pt) using MgAl (2/1) as support. Although most of the C4 obtained with MgAl (2/1) is butanol, the presence of dehydrogenation active metals could enhance the enolization of crotonaldehyde or butanal prevailing over the total hydrogenation of these intermediates. Improving the hydrogenation, not only the alcohols selectivity but also the conversion is expected to increase reducing the relevance of adsorption processes. In all the cases, a theoretical 1 wt% of metal loading is used, to limit the interference on the support properties and to guarantee the appropriate metal dispersion. Main results related to the catalytic characterization are summarized in Table 4.

The specific metal loadings measured by ICP-MS (>0.93) indicate a high similarity between materials, discarding any effect of this parameter in the discussion of their catalytic behavior. In the same way, TEM microscopy (Fig. S6) reveals the presence of metal particles in the range of 4–5 nm, with a very similar dispersion of Pd and Pt (29–30%), being slightly lower in the case of Cu (24%), and a bit higher with Ru (38%). As expected, the presence of metal particles partially modifies the acidity and basicity of the support. Thus, all the materials show a decrease in the acidity (more relevant in the cases of weak and medium sites), as well as the corresponding decrease (with the exception of Ru/MgAl) in the basicity. The slight increase in the strong acidity of some materials (Cu and Ru) is explained by the strong acid character of metal ions, suggesting the coexistence of some cations on the surface, together with the metal particles visualized by TEM. To sum up, the characterization of these materials corroborates a partial alteration in the morphological and chemical properties of the support, justifying the need of working with low amounts of metal (1%) to minimize these effects and guarantee a correct analysis of these effects.

Table 4
Surface and physicochemical properties of the different metal modified Mg/Al (2/1) catalysts. Results corresponding to N_2 physisorption and NH_3 and CO_2-TPD.

	MgAl (2/1)	Cu/MgAl (2/1)	Ru/MgAl (2/1)	Pd/MgAl (2/1)	Pt/MgAl (2/1)
S_{BET} ($m^2 \cdot g^{-1}$)	179	173	236	151	77
d_p (nm)	8	8	8	8	10
Total acidity ($\mu mol \cdot g^{-1}$)	**1857**	**1491**	**1565**	**998**	**1036**
Weak (<250ºC)	726	436	743	384	377
Medium	959	606	231	469	512
Strong (>500ºC)	172	449	591	145	147
Total basicity ($\mu mol \cdot g^{-1}$)	**716**	**598**	**852**	**555**	**735**
Weak (<250ºC)	185	324	315	250	178
Medium	441	210	536	291	286
Strong (>500ºC)	90	65	0	14	271
Metal loading (%)	–	0.96	0.98	0.93	0.94
Metal dispersion (%)	–	24.2	37.8	29.2	29.9
Metal particle size (nm)	–	5.2	4.0	4.9	4.9

Fig. 6 compares the main results, in terms of ethanol conversion and product distribution. A clear improvement in the conversion is observed with Pd (3.4%) and mainly Cu/MgAl, reaching a final value of 6.8% (2.68 g of EtOH converted per g of catalyst and hour). This value is higher than those reported in the literature for systems with similar metal loading, even working with catalyst/reactant mass ratios four times higher [14,21]. The closest value published (2.46 g/g·h) corresponds to a catalyst involving Cu and Ni, two metals for dehydrogenation [48]. This supports the hypothesis of the high relevance of the first dehydrogenation on the global reaction.

The conversion is proportional to the weak-strength basic/acid pairs (see Fig. 7a) for all the materials expect for the Cu/MgAl, material with which the conversion is almost double than the expected one. This result indicates that the presence of reduced metals (Pd, Pt, Ru) is not relevant for conversion, only affecting to the product distribution, whereas the well-known dehydrogenation activity of Cu plays a key role in the reaction.

All the bifunctional catalysts produce mixtures enriched in acetaldehyde. This suggests that the condensation activity is affected by the metals. However, C6s and C8s reach more relevance, representing 14.9% with the parent support but 25% with Pt. These data, together with the continuous increasing trend observed in their profiles (shown in Fig. S7-10), indicate that the dehydrogenation activity is faster than the consumption by condensation of the acetaldehyde and longer times are expected to produce an enrichment in the heavy fractions. Lateral reactions are also favored by bifunctional catalysts, obtaining a ratio between the sum of esters and ethers and the sum of all the compounds involved in the Guerbet route that increases from 0.06 of the original MgAl (2/1) to 0.18, 0.28, 0.15, and 0.23, with Cu, Ru, Pd, and Pt, respectively.

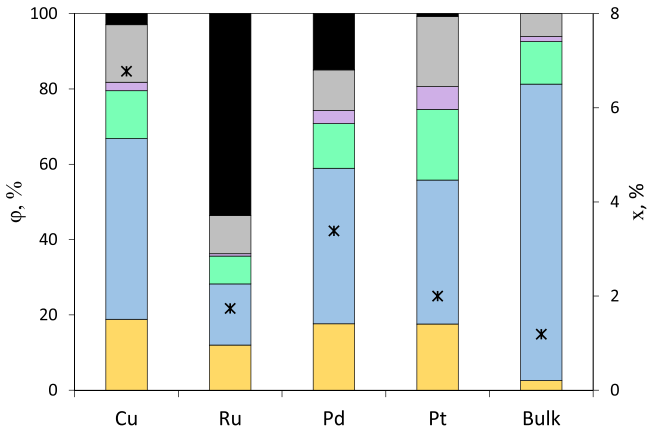

Fig. 6. Products distribution after 8 h of ethanol liquid-phase condensation with different bifunctional catalysts. Legend: C2 (yellow), C4 (blue), C6 (green), C8 (violet), undesired compounds (grey), and undetected gases (black). Conversions indicated with asterisks.

The total selectivity to target compounds (alcohols) decreases from 79.1% (MgAl (2/1)) to 49.7%, 12.3%, 42.6%, and 42.7% (Cu, Ru, Pd, and Pt). These values are justified since the presence of heavier compounds hinders the hydrogenation in absence of reducing atmosphere, using the hydrogen removed during dehydrogenation that is not desorbed from the liquid ethanol. Thus, the MPV hydrogenation mechanism prevails, the total selectivity of alcohols being proportional to medium-strength acidity, as illustrated in Fig. 7b. However, interesting conclusions can be extracted by analyzing the distribution of these alcohols, shown in Fig. 8.

Butanol represents almost 100% of the alcohols observed with MgAl (98.7%), whereas the presence of metal nanoparticles produces a significant decrease in this percentage in favor of heavier fractions (in good agreement with the higher conversions). Thus, the alcohol distribution obtained with Cu/MgAl indicates 81.9% of butanol, with 15.7% of C6 alcohols and 2.4% of C8. The same analysis reports 88.5%, 8.3%, and 2.1% of butanol, C6, and C8 alcohols with Ru/MgAl; 77.6%, 18.3% and 4.1%, respectively, with Pd/MgAl; and 69.5%, 22.2%, and 8.3%, with Pt/MgAl. This last catalyst presents a very interesting hydrogenation capacity combined with the highest selectivity for unsaturated compounds. However, these results are not significantly different from those reached with Cu/MgAl, a catalyst that has a conversion 240% higher than Pt/MgAl. In global terms, and considering that Cu/MgAl produces the second higher alcohol total selectivity, this material is chosen as the optimum one among the tested in this screening.

4. Conclusions

The activity of different catalysts in the ethanol liquid-phase condensation reveals a strong influence of acidity and basicity of the materials, global results being limited by the dehydrogenation activity. This limitation is more evident as the size of the molecule that must undergoes dehydrogenation increases, in such a way that dehydrogenation metal phases are required to promote the production of C6s and C8s and their subsequent alcohols. These compounds, not observed in gas-phase, are produced in the condensed one since the hydrogenation rate is significantly slower, promoting successive condensations.

Some materials are reactivated by the rehydration of aluminum oxide phases with the water in situ produced. However, the competitive adsorption of water and ethanol on the acid sites produces a decrease in the dehydrogenation activity in presence of small percentages of free water (2.5, 5%), conditioning the complete evolution of the reaction.

Cu is identified as the optimum metal observing a synergetic effect with the MgAl (2/1) support. 1% Cu/MgAl (2/1) allows a conversion almost five times higher than the one obtained with the parent material, producing almost 50% of alcohols with a selectivity distribution enriched in C6s and C8s (18.1%). These results involve a significant improvement in this field, supporting the liquid-phase production of heavy alcohols from ethanol with low catalytic loadings.

CRediT authorship contribution statement

Laura Faba: Methodology, Supervision, Data curation, Writing – original draft. **Jennifer Cueto:** Investigation, Data curation, Writing – original draft. **Mª Ángeles Portillo:** Investigation, Resources. **Ángel L. Villanueva Perales:** Formal analysis, Writing – review & editing. **Salvador Ordóñez**: Conceptualization, Supervision, Formal analysis,

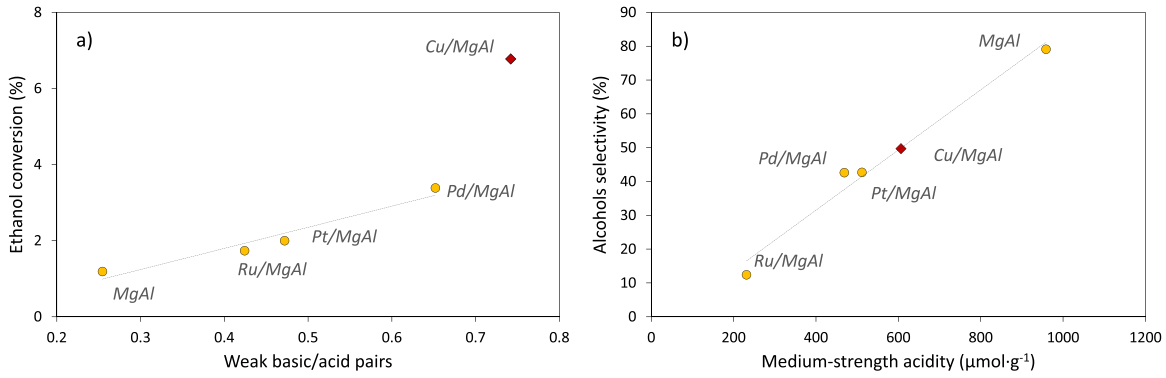

Fig. 7. Analysis of a) ethanol conversion and, b) alcohols selectivity as a function of the catalytic characterization properties.

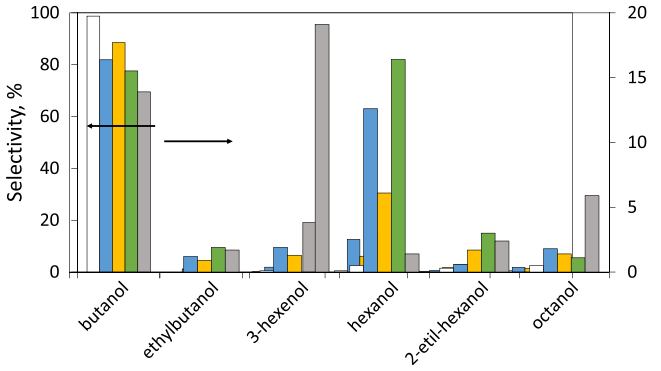

Fig. 8. Alcohol distribution obtained after 8 h of ethanol liquid-phase condensation catalyzed by MgAl (2/1) (white); Cu/MgAl (blue); Ru/MgAl (yellow); Pd/MgAl (green); and Pt/MgAl (grey). (Butanol selectivity in left axis; all the other alcohols in the right axis).

Writing – review & editing. **Fernando Vidal:** Supervision, Funding acquisition.

Declaration of Competing Interest

The authors declare that they have no known competing financial interests or personal relationships that could have appeared to influence the work reported in this paper.

Data availability

Data will be made available on request.

Acknowledgments

This work has been carried out in the framework of the Project BIOC4+ (PY18-RE-0040) funded by Junta de Andalucía and European Union (ERDF funds). Authors would like to acknowledge the technical support provided by Servicios Científico-Técnicos de la Universidad de Oviedo.

Appendix A. Supporting information

Supplementary data associated with this article can be found in the online version at doi:10.1016/j.apcata.2022.118783.

References

[1] W. Michaels, H. Zhang, W.L. Luyben, J. Baltrusaitis, Biomass Bioenerg. 109 (2018) 231–238, https://doi.org/10.1016/j.biombioe.2017.12.031.
[2] V. Narisetty, R. Cox, N. Willoughby, E. Aktas, B. Tiwari, A.S. Matharu, K. Salonitis, V. Kumar, Sust. Eng. Fuel 5 (2021) 4842–4849, https://doi.org/10.1039/d1se00575h.
[3] E.S. Olson, R.K. Sharma, T.R. Aulich, Appl. Biochem. Biotechnol. 115 (2004) 913–932, https://doi.org/10.1385/ABAB:115:1-3:0913.
[4] S. Logo, A. Onda, K. Iwasa, A. Fukuoka, J. Yanigisawa, J. Catal 296 (2012) 24–30, https://doi.org/10.1016/j.jcat.2012.08.019.
[5] J. Quesada, L. Faba, E. Díaz, S. Ordóñez, Appl. Catal. A 542 (2017) 271–281, https://doi.org/10.1016/j.apcata.2017.06.001.
[6] P. Benito, A. Vaccari, C. Antonetti, D. Licursi, N. Schiarioli, E. Rodriguez-Castellón, A.M. Raspolli Galleti, J. Clean. Prod. 209 (2019) 1614–1623, https://doi.org/10.1016/j.jclepro.2018.11.150.
[7] D.H. Jiang, G.Q. Fang, Y.Q. Tong, X.Y. Wu, Y.F. Wang, D.S. Hong, W.H. Leng, Z. Liang, P.X. Tu, L. Liu, K.Y. Xu, J. Ni, X.N. Li, A.C.S. Catal 8 (2018) 11973–11978, https://doi.org/10.1021/acscatal.8b04014.
[8] J. Quesada, L. Faba, E. Díaz, S. Ordóñez, Appl. Catal. A 563 (2018) 64–72, https://doi.org/10.1016/j.apcata.2018.06.037.
[9] T. Moteki, D.W. Flaherty, ACS Catal. 6 (2016) 4170–4183, https://doi.org/10.1021/acscatal.6b00556.
[10] P.T. Patil, D.P. Liu, Y. Liu, J. Chang, A. Borgna, Appl. Catal. A 543 (2017) 67–74, https://doi.org/10.1016/j.apcata.2017.05.025.
[11] J. Quesada, R. Arriola-Tapia, L. Faba, E. Díaz, V.M. Rentería-Sánchez, S. Ordóñez, Appl. Catal. A 551 (2018) 23–33, https://doi.org/10.1016/j.apcata.2017.12.004.
[12] K. Inui, T. Kurabayashi, S. Sato, J. Catal. 212 (2002) 207–215, https://doi.org/10.1016/jcat.2002.3769.
[13] T. Riitonen, V. Eta, S. Hyvärinen, L.J. Jönssson, J.P. Mikkola, Adv. Chem. Eng. (2013) 1–73, https://doi.org/10.1016/B978-0-12-386505-2.00001-8.
[14] I.-C. Marcu, D. Tichit, F. Fajula, N. Tanchoux, Catal. Today 147 (2009) 231–238, https://doi.org/10.1016/j.cattod.2009.04.004.
[15] T. Riittonen, K. Eranen, P. Marki-Arvela, A. Shchukarev, A.-R. Rautio, K. Kordas, N. Kumar, T. Salmi, J.-P. Mikkola, Renew, Energ 74 (2015) 369–378, https://doi.org/10.1016/j.renene.2014.08.052.
[16] T. Riittonen, T. Salmi, J.P. Mikkola, J. Warna, Top. Catal. 57 (2014) 1425–1429, https://doi.org/10.1007/s11244-014-0314-4.
[17] T. Riittonen, E. Toukoniitty, D.K. Madnani, A.R. Leino, K. Kordas, M. Szabo, A. Sapi, K. Arve, J. Wärna, J.P. Mikkola, Catalysts 2 (2012) 68–84, https://doi.org/10.3390/catal2010068.
[18] S. Marx, B. Ndaba, Biofuels 12 (2021) 861–868, https://doi.org/10.1080/17597269.2018.1554947.
[19] K.J. Pellow, R.L. Wingad, D.F. Wass, Catal. Sci. Technol. 7 (2017) 5161–5167, https://doi.org/10.1039/c7cy01553d.
[20] H.S. Ghaziaskar, C. Xu, R.S.C. Adv 3 (2013) 4271–4280, https://doi.org/10.1039/c3ra00134b.
[21] I.-C. Marcu, N. Tanchoux, F. Fajula, D. Tichit, Catal. Let. 143 (2013) 23–30, https://doi.org/10.1007/s10562-012-0935-9.
[22] I. Nezam, L. Peereboom, D.J. Miller, J. Clean. Prod. 209 (2019) 1365–1375, https://doi.org/10.1016/j.jclepro.2018.10.276.
[23] T.L. Jordison, C.T. Lira, D.J. Miller, Ind. Eng. Chem. Res. 54 (2015) 10991–11000, https://doi.org/10.1021/acs.iecr.5b02409.
[24] R.T. Clark, US. Patent 3972952 (1976).
[25] O.V. Larina, K.V. Valihura, P.I. Kyriienko, N.V. Vlasenko, D.Y. Balakin, I. Khalakhan, T. Cendak, S.O. Soloviev, S.M. Orlyk, Appl. Catal. A 588 (2019), 117265, https://doi.org/10.1016/j.apcata.2019.117265.
[26] A.D. Patel, S. Telalović, J.H. Bitter, E. Worrell, M.K. Patel, Catal. Today 239 (2015) 56–79, https://doi.org/10.1016/j.cattod.2014.03.070.
[27] C.A. Hamilton, S.D. Jackson, G.J. Kelly, Appl. Catal. A 263 (2004) 63–70, https://doi.org/10.1016/j.apcata.2003.12.009.
[28] Y. Li, X. Liu, H. An, X. Zhao, Y. Wang, Ind. Eng. Chem. Res. 55 (2016) 6293–6299, https://doi.org/10.1021/acs.iecr.6b00828.
[29] N. Liang, X. Zhang, H. An, X. Zhao, Y. Wang, Green. Chem. 17 (2015) 2959–2972, https://doi.org/10.1039/c5gc00223k.
[30] A.V. Chistyakov, S.A. Nikolaev, P.A. Zharova, M.V. Tsodikov, F. Manenti, Energy 166 (2019) 569–576, https://doi.org/10.1016/j.energy.2018.10.071.
[31] O.M. Perrone, M.R. Siqueira, G. Metzker, D.C. Oliveira Lisboa, M. Boscolo, Env. Prog, Sust. Energ. 40 (2021), e13541, https://doi.org/10.1002/ep.13541.

[32] C.R. Ho, S. Shylesh, A.T. Bell, A.C.S. Catal 6 (2016) 939–948, https://doi.org/10.1021/acscatal.5b02672.
[33] S. Ogo, A. Onda, M. Y. Iwasa, K. Hara, A. Fukuoka, K. Yanagisawa, J. Catal. 296 (2012) 24–30, https://doi.org/10.1016/j.jcat.2012.08.019.
[34] S. Ogo, A. Onda, K. Yanagisawa, Appl. Catal. A 402 (2011) 188–195, https://doi.org/10.1016/j.apcata.2011.06.006.
[35] N.M. Eagan, M.D. Kumbhalkar, J.S. Buchanan, J.A. Dumesic, G.W. Huber, Nat. Rev. Chem. 3 (2019) 223–249, https://doi.org/10.1038/s41570-019-0084-4.
[36] J.T. Scanlon, D.E. Willis, J. Chromatogr. Sci. 23 (1985) 333–340, https://doi.org/10.1093/chromsci/23.8.333.
[37] M. Schmal, D.V. Cesar, M.M.V.M. Souza, C.E. Guarido, Can. J. Chem. Eng. 89 (2011) 1166–1175, https://doi.org/10.1002/cjce.20597.
[38] D.L. Carvalho, L.E.P. Borges, L.G. Appel, P.R. de la Piscina, N. Homs, Catal. Today 213 (2013) 115–121, https://doi.org/10.1016/j.cattod.2013.03.034.
[39] Z. Wang, G. Lu, Y. Guo, Y. Guo, X.Q. Gong, ACS Sust, Chem. Eng. 4 (2016) 1591–1601, https://doi.org/10.1021/acssuschemeng.5b01533.
[40] S. Somrani, M. Banu, M. Jemal, C. Rey, J. Solid, State Chem. 178 (2005) 1337–1348, https://doi.org/10.1016/j.jssc.2004.11.029.
[41] C.K.S. Choong, L. Huang, Z. Zhong, J. Lin, L. Hong, L. Chen, Appl. Catal. A 407 (2011) 155–162, https://doi.org/10.10169/j.apcata.2011.08.038.
[42] D. Shee, G. Deo, Catal. Today 325 (2019) 25–32, https://doi.org/10.1016/j.cattod.2018.06.003.
[43] A.V. Chistyakov, S.A. Nikolav, P.A. Zharova, M.V. Tsodikov, F. Manenti, Energy 166 (2019) 569–576, https://doi.org/10.1016/j.energy.2018.10.071.
[44] M.M. Rahman, S.D. Davidson, J. Sun, Y. Wang, Top. Catal. 59 (2016) 37–45, https://doi.org/10.1007/s11244-015-0503-9.
[45] T.L. Jordison, L. Peereboom, D.J. Miller, Ind. Eng. Chem. Res. 55 (2016) 6579–6585, https://doi.org/10.1021/acs.iecr.6b00700.
[46] G.M.C. Gonzalez, P. Concepcion, A.L.V. Perales, A. Martinez, M. Campoy, F. Vidal-Barrero, Fuel Process. Technol. 193 (2019) 263–272, https://doi.org/10.1016/j.fuproc.2019.04.036.
[47] J. Quesada, L. Faba, E. Díaz, S. Ordóñez, ChemCatChem 10 (2018) 3583–3592, https://doi.org/10.1002/cctc.201800517.
[48] Z. Sun, A.C. Vasconcelos, G. Bottari, M.C.A. Stuart, G. Bonura, C. Cannilla, F. Frusteri, K. Barta, ACS Sustain. Chem. Eng. 5 (2017) 1738–1746, https://doi.org/10.10021/acssuschemeng.6b02494.